Universiteit
Leiden
The Netherlands

Stressed-out stress systems: dysregulated stress-systems in the pathophysiology of stress-related disorders

Bauduin, S.E.E.C.

Citation

Bauduin, S. E. E. C. (2022, November 23). *Stressed-out stress systems: dysregulated stress-systems in the pathophysiology of stress-related disorders*. Retrieved from https://hdl.handle.net/1887/3487160

Version:	Publisher's Version
License:	Licence agreement concerning inclusion of doctoral thesis in the Institutional Repository of the University of Leiden
Downloaded from:	https://hdl.handle.net/1887/3487160

Note: To cite this publication please use the final published version (if applicable).

Chapter 7

Potential associations between immune signaling genes, deactivated microglia, and oligodendrocytes and cortical gray matter loss in patients with long-term remitted Cushing's disease

S.E.E.C. Bauduin[1,2], I.L.B. den Rooijen , M. Meijer[3], S.J.A. van der Werff[1,2], A. Keo[4,6], O. Dzyubachyk[7], A.M. Pereira[2,5], E.J. Giltay[1], N.J.A. van der Wee[1,2], O.C. Meijer[2,5], A. Mahfouz[4,6,8]

[1]Department of Psychiatry, Leiden University Medical Center (LUMC), Leiden
[2]Leiden Institute for Brain and Cognition, Leiden
[3]Department of Human Genetics, Cognition and Behaviour, Donders Institute for Brain, Radboud University Medical Center, Nijmegen
[4]Leiden Computational Biology Center, Leiden University Medical Center, Leiden
[5]Department of Medicine, Division of Endocrinology, Leiden University Medical Center, Leiden
[6]Delft Bioinformatics Lab, Delft University of Technology, Delft
[7]Department of Radiology, Division of Image Processing, Leiden University Medical Center, Leiden
[8]Department of Human Genetics, Leiden University Medical Center, Leiden

Psychoneuroendocrinology 132 (2021) 105334

Abstract

Introduction

Cushing's disease (CD) is a rare and severe endocrine disease characterized by hypercortisolemia. Previous studies have found structural brain alterations in remitted CD patients compared to healthy controls, specifically in the anterior cingulate cortex (ACC). However, potential mechanisms through which these persistent alterations may have occurred are currently unknown.

Methods

Structural 3T MRI's from 25 remitted CD patients were linked with gene expression data from neurotypical donors, derived from the Allen Human Brain Atlas. Differences in gene expression between the ACC and an unaffected control cortical region were examined, followed by a Gene Ontology (GO) enrichment analysis. A cell type enrichment analysis was conducted on the differentially expressed genes, and a disease association enrichment analysis was conducted to determine possible associations between differentially expressed genes and specific diseases. Subsequently, cortisol sensitivity of these genes in existing datasets was examined.

Results

The gene expression analysis identified 300 differentially expressed genes in the ACC compared to the cortical control region. GO analyses found underexpressed genes to represent immune function. The cell type specificity analysis indicated that underexpressed genes were enriched for deactivated microglia and oligodendrocytes. Neither significant associations with diseases, nor evidence of cortisol sensitivity with the differentially expressed genes were found.

Discussion

Underexpressed genes in the ACC, the area vulnerable to permanent changes in remitted CD patients, were often associated with immune functioning. The specific lack of deactivated microglia and oligodendrocytes implicates protective effects of these cell types against the long-term effects of cortisol overexposure.

1. Introduction

Cushing's disease (CD) is a rare and severe endocrine disease caused by a pituitary adrenocorticotropic hormone (ACTH) producing adenoma. The excessive ACTH secretion stimulates the adrenal glands to produce excessive amounts of glucocorticoids (Newell-Price et al., 2006). In healthy individuals, increases in free circulating cortisol levels inhibit ACTH secretion (i.e. the negative feedback loop). In CD patients this feedback loop is impaired, resulting in increased levels of glucocorticoids or hypercortisolism, affecting numerous organs, including the brain.

Cortisol is a pivotal mediator of the stress response (De Kloet et al., 2005). Hypercortisolism has been associated with severe physical, psychological, and cognitive impairments, resulting in a substantial deterioration in quality of life (Forget et al., 2000; Leon-Carrion et al., 2009; Michaud et al., 2009; Newell-Price et al., 2006; Nieman and Ilias, 2005; Starkman et al., 1986). Regarding the psychological and cognitive impairments, stress-related symptoms such as anxiety, depression, and mania commonly present alongside CD, as do cognitive deficits within the domains of reasoning, verbal learning, language performance, visual and spatial information processing, and memory impairments (Newell-Price et al., 2006). These symptoms all support the notion that acute as well as prolonged exposure to excessive cortisol adversely affect the central nervous system (CNS).

Current treatment strategies abrogate excessive cortisol signaling and offer substantial alleviation of several associated symptoms, but certain debilitating psychological symptoms often persist, even after long-term remission. These persistent impairments are predominantwithin the domains of cognitive function and psychopathology (Andela et al., 2013; Bas-Hoogendam et al., 2015; Dorn et al., 1995; Pereira et al., 2010; Pivonello et al., 2015; Ragnarsson et al., 2012; Sonino and Fava, 2001; Tiemensma et al., 2010). Alongside these persevering symptoms, structural changes in the brain have been found in long-term remitted CD patients in comparison to healthy controls. Specifically, magnetic resonance imaging (MRI) studies have reported widespread reductions of white matter integrity, as well as smaller anterior cingulate cortex (ACC) volumes (Andela et al., 2013; van der Werff et al., 2014). However, MRI studies alone cannot offer sufficient insight into the underlying biological processes that lead to the observed reductions in white matter integrity and atrophy in the ACC in remitted CD patients.

The ACC, as part of the limbic system, is a relevant brain area to explore further as it is involved in various cognitive and emotional functions, many of which can be persistently impaired after cure of CD. Andela et al. (2013) offered the hypothesis that intrinsic impairments and alterations in connectivity and/or biochemistry of these brain regions may have caused the structural differences observed in remitted CD patients. Such underlying biological processes could be further explored by combining information obtained from high resolution MRI scans with whole genome mRNA expression data derived from the Allen Human Brain Atlas (AHBA), a multi-modal atlas mapping gene expression across the healthy human brain (Hawrylycz et al., 2012). The comparison of regional correlations between gene expression and the MRI data may provide a better insight into which genes are likely to interact with hypercorticolism resulting in structural brain changes.

In the present study, we explore potential mechanisms through which the structure of the ACC changes when exposed to prolonged endogenous cortisol excess, by linking information derived from high resolution MRI scans with gene expression data derived from the AHBA. We examined the differential gene expression in the ACC in comparison to a control region. Subsequently, the functionality of the differentially expressed genes was characterized by means of a Gene Ontology (GO) enrichment analysis. A cell type enrichment analysis investigated whether the differentially expressed genes were enriched for certain cell type markers, followed by a disease enrichment association analysis to assess whether the differentially expressed genes were associated with any specific group of diseases. Finally, we explored the cortisol sensitivity of the differentially expressed genes.

2. Methods

2.1. Subjects and data acquisition

Data were derived from a study conducted with long-term remitted CD patients and healthy controls, aged between 18 and 60 years old. A detailed explanation of this study protocol has previously been published elsewhere (Andela et al., 2013). In brief, a total of 25 long-term remitted CD patients and 25 age-, gender-, and education matched healthy controls were included in this sample. The diagnosis of CD had been confirmed in accordance with previously described international guidelines (Tiemensma et al., 2010). All CD patients underwent transsphenoidal surgery (n = 25). Six patients received additional post-operative radiotherapy and two other patients underwent bilateral adrenalectomy. All participants were right-handed, had no contraindications for the MRI scanner, and were psychopathology-,

drug-, and alcohol abuse-free with the exception of one patient who used antidepressants. Patients who remained glucocorticoid dependent after surgery (in addition to the two patients that received postoperative radiotherapy) received hydrocortisone replacement (on average 20 mg/daily in two to three dosages), and were evaluated twice per year. The estimated disease duration was determined retrospectively using patient recall of earliest physical and/or psychological symptoms of CD. Remission duration was calculated from the date of transsphenoidal surgery, whereby remission was confirmed by multiple biochemical test outcomes (e.g. normal midnight salivary cortisol (below 5.7 nmol/L, normal overnight suppression of serum cortisol levels (<50 nmol/L) by dexamethasone (1 mg), and normal 24-h urinary free cortisol excretion rates (<220 nmol/24 h), and by means of clinical evaluation. Prior to being included is the study, persistent biochemical remission of hypercortisolism was confirmed by means of the abovementioned diagnostic tests. Informed consent was obtained from all participants and the study protocol was approved by the Leiden University Medical Center ethics review board.

Images were acquired by a Philips 3.0T Achieva MRI scanner (Philips Medical Systems, Best, The Netherlands; software version 3.2.1) using a 32-channel SENSE (sensitivity encoding) head coil. Anatomical images were obtained by means of a sagittal three-dimensional gradient-echo T1-weighted sequence (repetition time 9.8 ms, echo time 4.6 ms, matrix size 256 × 256, voxel size 1.17 × 1.17 × 1.2 mm3, 140 slices, scan duration 4:56 min), as a part of a larger scan protocol. All anatomical images were examined by a neuroradiologist blinded for participants clinical details. No further macroscopic abnormalities were found in either patients or controls, with the exception of the effects of post-transsphenoidal surgery and incidental age-related white matter hyperintensities.

2.2. Behavioral and clinical severity assessments

The Montgomery-Åsberg Depression Rating Scale (MADRS; Montgomery and Åsberg, 1979), and the Inventory of Depression Symptomatology (IDS; Rush et al., 1986) were used to assess the severity of depressive symptoms. The MADRS was assessed by an interviewer, all other scales were self-reported. Anxiety was evaluated using the Beck Anxiety Inventory (BAI; Beck et al., 1988), the social phobia, blood injury phobia, and agoraphobia subscales, the total score of the Fear Questionnaire (FQ; Marks and Mathews, 1979), and the Beck Anxiety Inventory (BAI; Beck et al., 1988). The Apathy Scale (AS) and the Irritability Scale (IS) were used to assess the severity of apathy and irritability, respectively (Starkstein et al., 2001; Chatterjee et al., 2005). Participants with total scores of more than 14 points were considered to

be apathetic or irritable. Failures in memory, perception, and motor function were assessed using the Cognitive Failure Questionnaire (CFQ; Broadbent et al., 1982), higher sum scores indicating greater symptom severity.

CD symptom severity (active and the remitted disease state) were established using the Cushing's Syndrome Severity Index (CSI; Sonino et al., 2000). The CSI score during active disease was assessed retrospectively. The remission score was based on the last annual evaluation. Total CSI scores were used for both active and remitted disease states. Scores on this index can range between 0 and 16, with higher total scores indicating greater symptom severity. The information necessary to score the CSI was obtained from the patient's medical records and clinical history. The index was scored by two independent raters who reached consensus in the case of discrepancy.

2.3. Allen Human Brain Atlas (AHBA)

The Allen Human Brain Atlas (AHBA) is a genome-wide transcriptional atlas of the pathology-free human brain, providing gene expression data derived from six healthy human brains between the ages of 24–57 (Hawrylycz et al., 2012, 2015). More than 500 regions were sampled from each hemisphere, and 19,992 genes were extracted using multiple probes. Microarray data were downloaded from the AHBA database and probes were mapped to genes as previously described (Keo et al., 2017). Z-scores for normalized gene expression levels from the AHBA were calculated separately for each of the six individual brains. A major strength of the AHBA is that the gene expression data is mapped to the Montreal Neurological Institute (MNI) space (Collins et al., 1998), a standardized phantom brain that can be used to compare neuroimaging data across different brains.

2.4. Mapping AHBA to MRI data

As described in more detail by Andela et al. (2013), structural data were analyzed using FSL-VBM (a voxel-based morphometry style analysis; FMRIB's software library; Smith et al., 2004). In this study, smaller gray matter volumes were found in a large part of the bilateral ACC in remitted CD patients in comparison with controls (617 voxels; $p < 0.05$, 2 mm isotropic). We selected this region as our region of interest (ROI). Throughout the manuscript the ROI will be referred to as the ACC. A control region was selected by identifying the cortical area that showed the least differences between healthy controls (HCs) and patients with remitted CD (Andela et al., 2013). This region was identified using t-statistic thresholds of 0.7 to 0.0001 and 0.0001 to 0.7 respectively, leading to a control region consisting of segments

of the dorsolateral prefrontal cortex (see Fig. 1). As these regions are anatomically distinct, there are likely to be functional differences between these regions. However, as this control region is anatomically adjacent to the ACC, anatomically driven transcriptional differences are consequently minimized (e.g. Huntenburg et al., 2018). The ABHA samples were then mapped to the ACC and control region based on their associated MNI coordinates.

2.5. Differential gene expression in the ACC

Differences in gene expression between regions were examined by comparing expression level of genes between the ACC to the control region by means of two-tailed independent t-tests. Genes were considered to be differentially expressed at a Benjamini-Hochberg (HB; Benjamini and Hochberg, 1995)-adjusted p-value of <0.05 and effect size of log2(fold-change) >1.

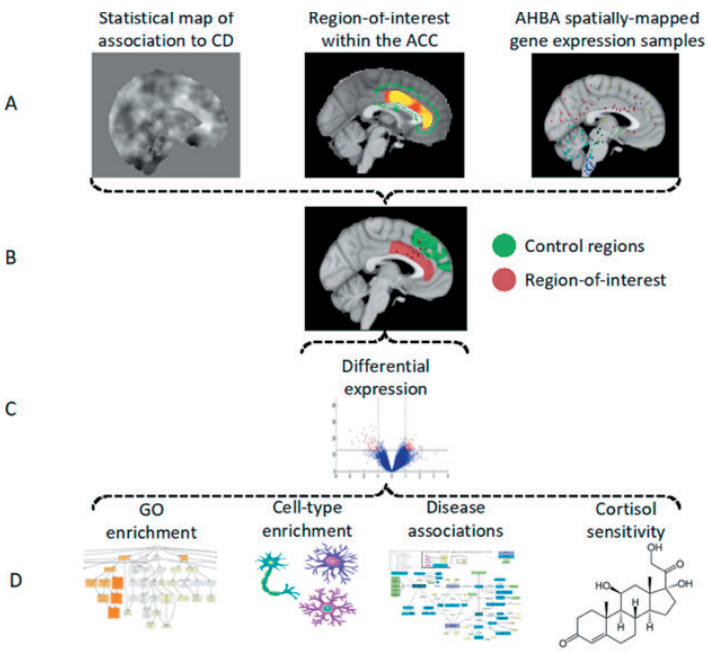

Figure 1. Study overview. (A) The Anterior Cingulate Cortex (ACC; region of interest) from our earlier study on grey matter volumes in patients with remitted Cushing's Disease (Andela et al., 2013) and the gene expression data derived from the AHBA (B) The identification of a control region (close in proximity to the ACC with a similar neuronal characteristic and showing the least differences to the ACC using a stringent threshold and the ROI mapped onto the AHBA gene expression data (C) Differential gene expression analysis (D) Enrichment or depletion for Gene ontology, cell type markers, disease associations, and cortisol sensitivity of differentially expressed genes.

2.6. Gene ontology (GO) enrichment analysis

To characterize the functionality of the differentially expressed genes, a Gene Ontology (GO) enrichment analysis was performed using GOrilla (Gene Ontology Enrichment Analysis and Visualization Tool), an online tool for identifying and visualizing enriched GO terms (Eden et al., 2009). Enrichment analysis was carried out for differentially over- and underexpressed genes. Gene symbols were used as identifiers, and a background list of the top 20% of genes with the highest expression level in the cortex was used to correct for non-selective ontology terms. GO terms with BH-corrected p-value <0.05 were considered significant. The following ontologies were used: 'GO: Biological Process' and 'GO: Molecular Function'.

2.7. Cell type enrichment analysis

In order to determine whether the differentially expressed genes were enriched for certain cell type markers, we conducted a cell type enrichment analysis. As our AHBA samples were located in the cortex region, a set of brain-region specific markers was used, focusing on 28 cell types (Mancarci et al., 2017). Markers were downloaded from the NeuroExpresso database (http://neuroexpresso.org) using markers from all brain regions. Entrez IDs of the mouse cell-type specific markers were converted to human homologs (homologene R-package version 1.4) and filtered for genes present in the AHBA dataset. Two markers with different mouse gene IDs (14972, H2-K1, microglial, and 15006, H2-Q1 serotonergic), were converted to the same human gene ID (3105, HLA-A), and therefore removed before analysis.

2.8. Enrichment analysis of disease-associated genes

A disease association enrichment analysis was conducted using disease gene sets from DisGeNET (http://www.disgenet.org/; Pi˜nero et al., 2016), in order to assess whether the differentially expressed genes are associated with any specific group of diseases. A table of 628,685 gene-disease associations covered 24,166 diseases that were tested for. Genes that were associated to waste-hip ratio and height were used in the analysis as control (i.e. non-disease) conditions (Lin et al., 2017; Heid et al., 2010).

2.9. Assessment of cortisol sensitivity of the ACC

We assessed whether the differentially expressed genes in our dataset were known to be regulated by glucocorticoids (GCs) in the brain, or in cell cultures derived from the central nervous system. We compared our list of differentially expressed genes with a list of genes that have been published by Juszczak and Stankiewicz (2018), who identified 113 genes that were consistently regulated by GCs across

studies. We also investigated GR and MR binding loci in the rat hippocampus under increased levels of corticosterone, the predominant glucocorticoid in this species (van Weert et al., 2017). Using these gene sets we identified GR-specific, MR-specific, as well as GR-MR overlapping DNA binding loci, which we used as potential target genes. Genes were converted from rat to human orthologues by use of the Toppfun Suite (Chen et al., 2009). In order to predict glucocorticoid sensitivity of the current differentially expressed genes, we assessed whether these target genes were enriched in the differentially expressed genes.

2.10. Enrichment statistics for GO, cell type, disease-associated genes and receptor binding

Enrichment statistics were determined based on Fisher's Exact Tests. Odds ratios (ORs) were calculated as a measurement of effect size with regard to the enrichments, with an OR > 1 and 0 < OR < 1 indicating enrichment and depletion, respectively. The BH method was used for all p-values to correct for multiple testing. A BH corrected p-value of <0.05 was considered to be significant.

2.11. Literature search on the differentially expressed genes

For all differentially expressed genes, a literature search was subsequently performed to determine previously found associations with normal and pathological processes or states. Furthermore, with regard to Cushing's Disease, specific known associations with the HPA-axis and/ or glucocorticoid responsiveness were investigated. This was done by means of a PubMed search using the following search term strategy: ("gene" [all fields]) AND ("HPA-axis" [all fields] OR "cortisol" [all fields] OR "glucocorticoid" [all fields] OR "GR" [all fields]). Interactions between genes were determined by means of searching gene pairs in Google Scholar.

3. Results

3.1. Patient characteristics

As previously published in Andela et al. (2013), mean disease duration was 7.9 years (ranging from 0.8 to 29.3 years), and mean duration of remission was 11.2 years (ranging from 0.8 to 37.0 years). The mean Cushing's Syndrome Severity Index score was 8.1 during the active period of CD, and 2.5 in the remitted CD-patients at the time of assessment (see Table 1 for further details).

Table 1. Demographics and psychometric data of remitted CD patients. Data are presented as mean ± standard deviation or number (%).

	CD patients (n = 25) Mean ± SD
Gender (female)	21(84%)
Age (years)	45 ± 8
Education	
Low	6 (24%)
Medium	12 (48%)
High	7 (28%)
Intracranial volume $\cdot 10^6$ (cm^3)	1.450 ± 0.163
MADRS	6.3 ± 5.5
Inventory of depressive Symptomatology	46.8 ± 13.0
Beck Anxiety Inventory	28.4 ± 5.7
Fear questionnaire	24.5 ± 17.4
Agoraphobia subscale	6.1 ± 7.9
Blood injury phobia subscale	6.2 ± 8.3
Social phobia subscale	12.2 ± 8.0
Irritability scale	12.1 ± 8.7
Total score >14	9 (36%)
Apathy scale	13.6 ± 6.6
Total score >14	11 (44%)
Cognitive failures questionnaire	38.0 ± 16.5
Disease duration (years)	7.9 ± 7.9
Duration of remission (years)	11.2 ± 8.2
Cushing's syndrome severity index	
Active phase (total)	8.1 ± 2.0
Remission phase (total)	2.5 ± 1.5

MADRS = Montgomery-Åsberg Depression Rating Scale.

3.2. Differentially expressed genes in the ACC in comparison to the control region

Given the small size of the regions analyzed, we aggregated all samples from the six donors in the AHBA. This led to a total of 31 samples in the ACC and 29 samples in the control region (see Table 2 for further details). Using a differential expression analysis, we identified 300 differentially expressed genes (BH-adjusted $p < 0.05$ and log2(fold- difference) >1 (see Fig. 1). Of these 300 differentially expressed

genes, 58 genes were overexpressed and 242 were underexpressed in the ACC in comparison to the control region (see Supplementary Tables S1 and S2) (Fig. 2). The top three most significantly overexpressed genes in the ACC in comparison to the control region were KIAA0748, also known as Thymocyte-expressed, positive selection-associated 1 (TESPA1; FDR = $4.80 \cdot 10^{-5}$, log2(FC) = 2.76), ONECUT2, One Cut Homeobox 2, (FDR = $1.94 \cdot 10^{-6}$, log2(FC) = 2.45), and CALML3, Calmodulin 3, (FDR = $3.44 \cdot 10^{-7}$, og2(FC) = 2.13).

Endothelial cell-specific molecule 1 (ESM1), Ubiquitin Specific Peptidase 54 (USP54), and Putative translationally-controlled tumor protein-like protein TPT1P8 (TPT1P8), also known as FKSG2, were the most underexpressed genes in the ACC in comparison to the control region (FDR = $6.43 \cdot 10^{-4}$, log2(FC) = 3.13; FDR = $5.28 \cdot 10^{-4}$, log2(FC) = -2.14; and FDR = $5.16 \cdot 10^{-3}$, log2(FC) = -2.13, respectively).

Table 2. Overview of samples from the six AHBA donors in the AAC and the control region.

	Donor 9861	Donor 10021	Donor 12876	Donor 14380	Donor 15496	Donor 15697	All donors
ACC	1	12	3	3	5	7	31
Control region	13	2	4	3	3	4	29

3.3. Functionality and cell type specificity of differentially expressed genes in the ACC

The GO term enrichment analysis found none of the enriched GO terms from the list of overexpressed genes to remain statistically significant after BH-adjustment for multiple testing. Genes with lower expression in the ACC compared to the control region were enriched for GO terms that were, amongst others, involved in synapse pruning, immune system processes, antigen processing, leukocyte-, macrophage- and (micro)glial activation. 34 GO-terms remained significant after correction for multiple testing at a BH adjusted p-value of < 0.05, although several of these terms were partially overlapping (see Supplementary Table S3 for further details). Based on the GO terms, the most frequently occurring genes involved in the processes (assigned to between 9 and 22 of the 34 significant GO-terms), were Triggering Receptor Expressed on Myeloid Cells 2 (TREM2), Integrin Subunit Alpha M (ITGAM), CD36, Interleukin 33 (IL33), Complement Component 3 (C3), human leukocyte antigen (HLA)-DRB1/-DQB1/-DMB/-DRB3/-DRB4 (all belonging to the HLA class II), and arachidonate 5-lipoxygenase (ALOX5; see Table 3 for further details and cell-types; Mancarci et al., 2017).

We then assessed whether a set of differentially expressed genes were particularly expressed in a cellular subtype and found that underexpressed genes were significantly enriched for deactivated microglia cells (7 markers; BH-corrected p-value = 0.001), and oligodendrocyte cells (12 markers, BH-corrected p-value = 0.036; see Supplementary Table S4 for a complete overview).

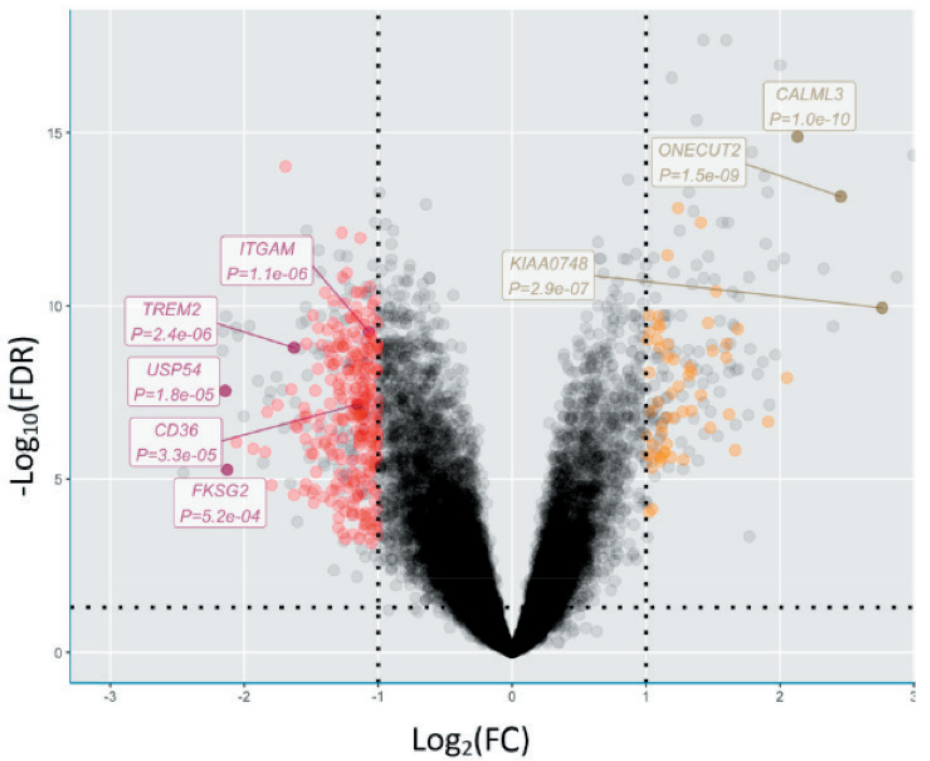

Figure 2. Genes significantly expressed after BH-correction at higher and lower levels (orange and red dots respectively) in the ACC relative to control regions are depicted on a volcano plot. Non-statistically significant differentially expressed genes in the cortical regions are depicted in black. (For interpretation of the references to color in this figure legend, the reader is referred to the web version of this article.)

Table 3. Overview frequency and cell type of often occurring genes in the 34 GO terms that remained significant after BH correction.

Gene	Number of times occurring	Cell type
ITGAM	23/34 (67.6%)	Microglia
TREM2	22/34 (64.7%)	Microglia
CD36	19/34 (55.9%)	Endothelial
IL33	16/34 (47.1%)	Oligodendrocytes and Astrocytes
C3	14/34 (41.2%)	Endothelial
HLA class II	12/34 (35.3%)	Microglia
ALOX5	9/34 (26.5%)	Microglia and Oligodendrocytes

3.4. Differentially expressed genes in the ACC are not associated with any diseases

Using disease gene sets from DisGeNet (Pi˜nero et al., 2016) containing 24,166 diseases, we tested the over- and underexpressed genes in the ACC for enrichment in psychiatric-brain diseases (e.g. MDD), -non-psychiatric brain diseases (e.g. Huntington's Disease), and non-disease traits (e.g. height and waist-hip-ratio). After BH-adjustment, no associations with any of these diseases remained significant.

3.5. Cortisol sensitivity of the ACC

Finally, we assessed whether the differentially expressed genes in our dataset were known to be regulated by glucocorticoids (GCs) in the brain or in cell cultures derived from the central nervous system. We compared our list of differentially expressed genes with a list of 113 genes that were found to be consistently regulated by GCs across studies (Juszczak and Stankiewicz, 2018). We found a non-significant overlap of one gene, namely LYVE1. We further compared our differentially expressed genes with genes that have been identified to be regulated by GCs and mineralocorticoids (MCs) in rats (van Weert et al., 2017), we found a non-significant overlap of the following genes: ASPA, CALML3, XCR1, and USP54, however not LYVE1.

4. Discussion

The current study aimed at exploring potential mechanisms underlying the persistent structural alterations of the ACC in patients with long-term remitted CD by linking information derived from high resolution MRI scans with gene expression data derived from the AHBA. By combining structural MRI data with gene expression data, we identified 300 differentially expressed genes in the ACC in comparison to the control region, several of which were immune signaling genes. In line with this

finding, the GO term enrichment analyses indicated that underexpressed genes were enriched for functionality involving, amongst others, immune functioning. Furthermore, cell type specificity analyses indicated that low-expressed genes were enriched for deactivated microglia and oligodendrocytes. No associations were found between the differentially expressed genes and specific diseases. Finally, our findings indicated no enrichment of glucocorticoid target genes in the ACC in comparison to the control region.

A potential limitation of our data study may be the relatively small ROI and sample sizes. This may make it difficult to detect certain effects due to a possible lack of power. Also, we are assessing gene expression levels in the healthy brain and not in those of remitted CD patients. This means that the differential expression may indicate vulnerability as present prior to CD, but tells us nothing about what the actual effects of cortisol exposure have been. Possible ways in which we could extend our findings to include the actual effects of cortisol are by extrapolating our current findings to existing mouse models (e.g. Drelon et al., 2016; Leccia et al., 2016), or by examining these areas in remitted CD patient brains post-mortem. However, material from patients with remitted CD will be extremely scarce. Furthermore, we used mouse data for our cell type enrichment analysis. There may therefore be a limited overlap with human data, thu replicating these findings in a robust human dataset is advisable. Finally, it is important to bear in mind that data derived from the CD patient population are cross-sectional, and we are therefore unable to determine whether these patients presented alterations in the ACC prior to the development of the disease.

The differential gene expression analysis indicated that KIAA0748, ONECUT2, and CALML3 were the most highly overexpressed genes in the ACC in comparison to the control region, and ESM1, USP54, and TPT1P8 were the most underexpressed. KIAA0748, ONECUT2, ESM1, USP54 have been found to be associated with various (auto-)immune diseases (e.g. Yao et al., 2015, 2018; Shen et al., 2019; Seo et al., 2020; Fraile et al., 2016; Jin et al., 2020; Xu et al., 2019; Li et al., 2019); and CALML3 has recently been found to affect the onset of Alzheimer's Disease (AD; Chen et al., 2019). The GO analysis conducted using the over- and underexpressed genes found that several of the most under- expressed genes, i.e. TREM2, ITGAM, CD36, IL33, HLA-DRB1/-DQB1/-DMB/-DRB3/-DRB4 (all belonging to the HLA class II), and ALOX5, were enriched for GO terms that were, amongst others, involved in immune-signaling. Interestingly, these genes have also been found to be associated with numerous (auto-)immune diseases, and strikingly all have been suggested to

be linked with AD. Specifically, variants in TREM2 have been strongly implicated in the pathogenesis of AD (Jonsson et al., 2013; Guerreiro et al., 2013). Moreover, a recent study investigating TREM2 knockout in human microglia cells in a xenograft mouse model using aggravated pathology found that TREM2 knockout microglia show lower viability, which is in line with a protective effect of this gene (McQuade et al., 2020). ITGAM has been proposed to be a candidate susceptibility locus for AD (Shulman et al., 2014), and CD36 gene polymorphisms have been associated with AD (Serý et al., 2017, 2020). Furthermore, IL33 has been identified as a candidate gene for AD (Chapuis et al., 2009), and several of the HLA class II genes, as well as ALOX5, have been found to be associated with AD (Lehmann et al., 2001; Wang et al., 2017; Serý et al., 2017).

The enrichment analysis for cortical cell-type markers found an underrepresentation of deactivated microglia in the ACC in comparison to the control region. Microglia form the first line of defense in the case of injury, disease, or invading pathogens in the CNS (Nimmerjahn et al., 2005), and actively partake in maintenance and plasticity of the adult CNS by secreting neurotrophic factors such as BDNF and cytokines (Parkhurst et al., 2013). They also refine the neuronal circuit by pruning axonal terminals and synapses (Parkhurst et al., 2013; Salter and Beggs, 2014). Microglia are generally known to polarize in two directions from a resting (M0) state: classical (M1) activation, known as the mediator of pro-inflammatory responses and alternative (M2) activation, which is responsible for resolution and repair (Zheng and Wong, 2019). The M2 microglial phenotypes are divided into M2a, M2b, and M2c (Franco and Fernandez-Suarez, 2015; Mantovani et al., 2004; Martinez et al., 2008). M2c microglia, also known as acquired deactivated microglia, have been found to be deactivated by adjacent cells through processes that are guided by local and systemic homeostatic signals, but are still poorly understood (Saijo and Glass, 2011; Starossom et al., 2012). M2c microglia have been found to participate in neuroprotection and to release certain anti-inflammatory cytokines (Zhang et al., 2018), as well as be involved in matrix deposition and tissue remodeling after inflammation has been downregulated (Mantovani et al., 2004). An underrepresentation of deactivated microglia in the ACC in the remitted CD patient population may be a possible explanation for the persevering alterations in the ACC, as well as the lasting impairments within a number of cognitive domains, as there are apparently few M2c microglia present to repair the possible 'damage' to this area.

Additionally, an underrepresentation of oligodendrocytes was found in the ACC

in comparison to the control region. Oligodendrocytes are largely responsible for the remyelination process (Alonso, 2000; Miyata et al., 2011), and damage to oligodendrocytes has been found to lead to a reduction or cessation in action potential velocity, leading to mental or physical disability (Karadottir and Attwell, 2007). Earlier animal studies have found an association between prolonged exposure to elevated corticosteroid levels and the inhibited proliferation of oligodendrocyte precursors throughout the white matter of the brain (Alonso, 2000; Miyata et al., 2011; Willette et al., 2012). A study investigating white matter integrity in the same patient population as the current study found reductions of fractional anisotropy (FA; a measurement used to assess white matter microstructure) values in nearly all of the white matter tracts throughout the brain (van der Werff et al., 2014). Although the study was cross-sectional and thus no causal conclusions can be drawn, all patients in this study had been exposed to hypercorticolism, leading to the authors suggestion that prolonged exposure to increased levels of cortisol causes reduced white matter integrity, either directly or indirectly. The lower FA values found can be linked to earlier findings showing that corticosterone treatment in mice can lead to an increased distance between nerve fibers in fiber tracts (Miyata et al., 2011). This is likely due to a consequence of direct glucocorticoid receptor activation in oligodendrocytes that lead to an increased branching of these cells and possibly to lower levels of myelination. In summary, the relative underrepresentation of oligodendrocytes present in the ACC may also offer a possible explanation for the persistent alterations in this area, as well as for the lasting cognitive impairments within the long-term remitted CD patient population. Oligodendrocytes are clearly affected during CD, and their underrepresentation in areas with long-term changes may indicate an insufficiently large buffer against the deleterious effects of excessive cortisol exposure.

With regard to the cortisol sensitivity of the ACC, our findings were opposite to what we had hypothesized. Earlier studies have found that MR and/or GR expression in the ACC is high (e.g. Hawrylycz et al., 2012), although this has not been found to be predictive of structural changes following chronic overexposure to glucocorticoids (Andela et al., 2013). Our findings indicated that the ACC does not seem to be enriched for glucocorticoid responsive genes, neither at the mRNA level, nor for DNA-binding loci for the GR and the MR.

In sum, these findings provide further insight into the possible molecular mechanisms underlying the vulnerability for persistent alterations in the ACC of patients with long-term remitted CD. Future studies should explore how oligodendrocyte and

deactivated microglia cell numbers confer vulnerability, and also characterize genes that are differentially expressed as a (long-term) consequence of the cortisol overexposure. Moreover, it would also be of interest to explore the epigenetic regulation of certain genes that were identified, as well as possible gene-environment interactions. It is important to note that although we have not studied the ACCs of remitted CD patients, the cortisol excess does meet a 'naïve' brain, of which some areas have been found to be vulnerable, whereas others have not. Our findings present differences in basal gene expression in vulnerable areas that define the initial situation in which vulnerability is inherent and well documented, and importantly, also tell us which genes are less likely to be part of this initial vulnerability as no differences were found in MR or GR expression, in HSD1, and in chaperones. Future further (experimental) studies in the ACCs of remitted patients using post-mortem tissue or in Cushing's mouse models (e.g. Amaya et al., 2021) are necessary to validate these findings. These findings may ultimately aid in developing novel treatments for stress-related disorders of the brain, and for CD patients in particular. In conclusion, we found that certain underexpressed genes in the ACC, a region afflicted in remitted CD, were often associated with immunology functioning, as well as a lack of deactivated microglia and oligodendrocytes in the ACC, implicating immune functioning in general and suggesting a protective role of these cell types in relation to the long-term effects of excess cortisol exposure in the brain.

Supplementary tables

Supplementary Table 1. Gene symbols of the 58 significantly overexpressed genes in the ACC compared to the control region

#	Gene	BH-adjusted p-value	Log2(FC)	#	Gene	BH-adjusted p-value	Log2(FC)
1	*KIAA0748*	4.8E-05	2.76	**31**	*VWC2L*	0.00020131	1.16
2	*ONECUT2*	1.9E-06	2.45	**32**	*ABHD12B*	0.0024415	1.15
3	*CALML3*	3.4E-07	2.13	**33**	*HIST1H1D*	0.00114689	1.15
4	*AC079341.1*	3.6E-4	2.05	**34**	*OSR1*	0.00313916	1.14
5	*CTXN3*	1.3E-3	1.91	**35**	*LOC100130811*	0.003082	1.14
6	*AC010087.3*	8.8E-05	1.68	**36**	*GSTA3*	0.00176408	1.12
7	*EPN3*	2.9E-3	1.67	**37**	*CREB3L3*	0.00144554	1.12
8	*ANKRD56*	1.0E-3	1.62	**38**	*CD70*	0.00360575	1.11
9	*C13orf39*	0.0001348	1.6	**39**	*GPX3*	0.00402601	1.11
10	*AC017096.1*	0.00020131	1.6	**40**	*AC116165.2*	0.00354063	1.11
11	*FOXP2*	2.9793E-05	1.52	**41**	*DKK2*	8.5189E-05	1.1
12	*AC109486.1*	0.00016555	1.5	**42**	*COL22A1*	0.00015231	1.1
13	*C6orf105*	0.00153647	1.48	**43**	*PRKG2*	7.8751E-05	1.1
14	*C7orf62*	7.4172E-05	1.46	**44**	*RP1-152L7.5*	0.00006123	1.09
15	*GEFT*	0.00060117	1.41	**45**	*P2RX6*	0.00073769	1.09
16	*C12orf64*	4.106E-06	1.41	**46**	*AC132186.2*	0.00012163	1.08
17	*AGPAT9*	0.00030327	1.34	**47**	*AC099797.1*	0.00355346	1.05
18	*TGFBI*	0.0009426	1.34	**48**	*LOC389831*	0.00251141	1.05
19	*C13orf16*	0.0002648	1.32	**49**	*LAIR2*	0.01596857	1.04
20	*KLF4*	0.00034234	1.31	**50**	*SGK493*	0.00487298	1.04
21	*KRT31*	0.00385741	1.28	**51**	*SHD*	0.0009461	1.03
22	*MUC20*	0.00096254	1.27	**52**	*SOCS7*	9.4916E-05	1.03
23	*TWIST2*	0.0004627	1.24	**53**	*SMYD1*	5.9949E-05	1.02
24	*CCL27*	2.7072E-06	1.24	**54**	*CRTAC1*	0.00031035	1.02
25	*C4orf22*	0.00021141	1.21	**55**	*GAL*	0.01758361	1.02
26	*C21orf110*	0.00115177	1.2	**56**	*LOC732327*	0.00340362	1.01
27	*IL7R*	0.0005663	1.19	**57**	*LOC646548*	0.0001214	1.01
28	*UBQLNL*	0.00359144	1.19	**58**	*CBLN1*	0.00196426	1
29	*SPTSSB*	0.00013992	1.16				
30	*ADRA2A*	1.0566E-05	1.16				

Supplementary Table 2. Gene symbols of significantly underexpressed genes in the ACC compared to the control region

#	Gene	BH-adjusted p-value	Log2(FC)	#	Gene	BH-adjusted p-value	Log2(FC)	#	Gene	BH-adjusted p-value	Log2(FC)
1	*ESM1*	0.000643	-3.131971	**33**	*CISH*	0.00147	-1.44661	**65**	*T*	0.000109	-1.297565
2	*USP54*	0.000528	-2.141561	**34**	*IGFN1*	0.000086	-1.446063	**66**	*OPALIN*	0.014623	-1.29625
3	*FKSG2*	0.005164	-2.127462	**35**	*PPM1F*	0.001065	-1.433598	**67**	*C18orf56*	0.020569	-1.293979
4	*XIRP1*	0.002321	-2.058309	**36**	*C3*	0.000141	-1.419813	**68**	*RP11-379K17.4*	0.003293	-1.292907
5	*AC217771.1*	0.002809	-1.932542	**37**	*HIST1H3J*	0.01126	-1.407132	**69**	*MAS1L*	0.00059	-1.292138
6	*NACAP1*	0.003092	-1.843889	**38**	*HCAR3*	0.002477	-1.398194	**70**	*CYTH4*	0.000135	-1.289241
7	*C7orf52*	0.000974	-1.828502	**39**	*CYBB*	0.000031	-1.395657	**71**	*LAPTM5*	0.000508	-1.289139
8	*LRRC37A16P*	0.008016	-1.796806	**40**	*APOL4*	0.00228	-1.395187	**72**	*IL27*	0.005852	-1.285478
9	*RP1-74M1.1*	0.000794	-1.751832	**41**	*C1QB*	0.000091	-1.377739	**73**	*PIK3R5*	0.000364	-1.278479
10	*ARHGAP6*	0.000001	-1.691281	**42**	*TNFAIP8L2*	0.000166	-1.366946	**74**	*DGKH*	0.003823	-1.275499
11	*RP13-102H20.1*	0.000506	-1.647887	**43**	*LINC00302*	0.000228	-1.364728	**75**	*GHRLOS*	0.001176	-1.271973
12	*TFAP2D*	0.010628	-1.628211	**44**	*PIK3AP1*	0.002772	-1.363659	**76**	*FCGR1B*	0.000006	-1.271732
13	*TREM2*	0.000152	-1.62805	**45**	*FCGR3A*	0.000764	-1.35984	**77**	*HLA-DRB1*	0.000661	-1.271721
14	*ADAMDEC1*	0.0014	-1.617845	**46**	*MGC34800*	0.012626	-1.353962	**78**	*FOLR2*	0.00002	-1.268012
15	*LRRC2*	0.001518	-1.603071	**47**	*ARVCF*	0.001631	-1.352179	**79**	*AC087645.1*	0.032335	-1.265673
16	*KCTD4*	0.00086	-1.552604	**48**	*LOC392145*	0.000383	-1.351312	**80**	*TTLL10*	0.013341	-1.265597
17	*LOC392352*	0.009379	-1.55075	**49**	*RIPK3*	0.009267	-1.342552	**81**	*LYZL1*	0.000148	-1.264477
18	*LOC100133583*	0.00111	-1.550365	**50**	*LOC493754*	0.003335	-1.341574	**82**	*SLC6A19*	0.001229	-1.26386
19	*EEF1A1P32*	0.00212	-1.543428	**51**	*CD300A*	0.00025	-1.339029	**83**	*HLA-DRB3*	0.002063	-1.261032
20	*TYMS*	0.007758	-1.538527	**52**	*PABPC3*	0.00215	-1.338831	**84**	*ZACN*	0.000145	-1.258726
21	*SLC5A12*	0.000135	-1.535445	**53**	*CCR1*	0.000149	-1.337939	**85**	*RHBDF2*	0.000042	-1.253818
22	*LOC100129104*	0.001131	-1.532802	**54**	*KCNQ1*	0.000075	-1.335623	**86**	*TTBK1*	0.01707	-1.24624
23	*UBE2NL*	0.003216	-1.500601	**55**	*VSIG4*	0.000039	-1.334618	**87**	*HELB*	0.03786	-1.24412
24	*PRSS36*	0.010023	-1.491626	**56**	*OLFML3*	0.00024	-1.332063	**88**	*C1QA*	0.000102	-1.242582
25	*ITGB2*	0.00006	-1.485939	**57**	*C10orf113*	0.009201	-1.317093	**89**	*UGT3A1*	0.000493	-1.238639
26	*ZNF962P*	0.003284	-1.483219	**58**	*CGB1*	0.007774	-1.314111	**90**	*CX3CR1*	0.000138	-1.238131
27	*HLA-DQB1*	0.013347	-1.481177	**59**	*SYK*	0.00015	-1.307994	**91**	*DOCK8*	0.000018	-1.234026
28	*C6orf124*	0.009127	-1.472043	**60**	*DHRS9*	0.00022	-1.304074	**92**	*CAPZA2*	0.007372	-1.231083
29	*HLA-DMB*	0.000524	-1.469848	**61**	*DUSIL*	0.001192	-1.301545	**93**	*LOC442293*	0.008759	-1.226626
30	*ASB18*	0.002411	-1.46391	**62**	*ALOX5*	0.000084	-1.300801	**94**	*GHSR*	0.000281	-1.226355
31	*DCAF8L2*	0.005493	-1.462881	**63**	*ICMT*	0.027369	-1.298883	**95**	*INHBC*	0.000286	-1.215329
32	*BHLHE22*	0.00028	-1.449861	**64**	*LINC00475*	0.000438	-1.298307	**96**	*POLR2A*	0.000063	-1.210874

Supplementary Table 2. Gene symbols of significantly underexpressed genes in the ACC compared to the control region (continued)

#	Gene	BH-adjusted p-value	Log2(FC)	#	Gene	BH-adjusted p-value	Log2(FC)	#	Gene	BH-adjusted p-value	Log2(FC)
97	*PAGE4*	0.000758	-1.209436	**129**	*CD36*	0.000782	-1.158675	**161**	*GKN1*	0.001195	-1.105922
98	*AC013553.1*	0.00106	-1.209154	**130**	*SIGLECP3*	0.000194	-1.155155	**162**	*DDX11L2*	0.000279	-1.105832
99	*PGDS*	0.000339	-1.203295	**131**	*CXXC11*	0.000708	-1.152977	**163**	*JAM3*	0.025207	-1.103934
100	*LOC149832*	0.000196	-1.199155	**132**	*TCP1P3*	0.010404	-1.152398	**164**	*KRTAP2-3*	0.000077	-1.103781
101	*ARPC3P3*	0.017512	-1.195586	**133**	*HLA-DRB4*	0.001093	-1.151974	**165**	*RNASE6*	0.00066	-1.103514
102	*GGNBP1*	0.003932	-1.193093	**134**	*ITGAX*	0.000249	-1.15014	**166**	*C13orf30*	0.007079	-1.102135
103	*CYTL1*	0.000065	-1.192892	**135**	*SLC18A1*	0.010783	-1.14557	**167**	*UG0898H09*	0.000332	-1.10062
104	*HRASLS2*	0.005571	-1.191768	**136**	*FCRLA*	0.002589	-1.143966	**168**	*KIF20A*	0.000172	-1.100388
105	*LOC652494*	0.001066	-1.191537	**137**	*KRTAP11-1*	0.002157	-1.14022	**169**	*CCL22*	0.000233	-1.099942
106	*AC084851.1*	0.01887	-1.191151	**138**	*CHIA*	0.000363	-1.139375	**170**	*AQP3*	0.000943	-1.099861
107	*ADAMTS14*	0.032904	-1.188686	**139**	*GLYATL1P4*	0.002337	-1.138993	**171**	*BTBD16*	0.024564	-1.092944
108	*GOLGA6C*	0.014243	-1.1872	**140**	*SSTR4*	0.01834	-1.138461	**172**	*HNRNPCL1*	0.020022	-1.092215
109	*BMF*	0.000097	-1.184658	**141**	*AL359392.2*	0.037019	-1.137754	**173**	*GPR142*	0.017669	-1.091013
110	*FSHB*	0.007905	-1.182569	**142**	*C5ORF27*	0.001052	-1.13442	**174**	*FLYWCH2*	0.003734	-1.090978
111	*PPBP*	0.001137	-1.181566	**143**	*FBP1*	0.000006	-1.133798	**175**	*ZDHHC19*	0.001603	-1.085208
112	*CYP2B7P1*	0.000172	-1.181442	**144**	*SUCNR1*	0.001047	-1.13215	**176**	*MRGPRD*	0.000129	-1.084214
113	*C4ORF10*	0.007289	-1.179522	**145**	*RBM22*	0.001528	-1.129837	**177**	*C1DP3*	0.000877	-1.083969
114	*CYB5R2*	0.011806	-1.174476	**146**	*PRSS58*	0.000031	-1.127723	**178**	*DCST2*	0.000584	-1.083159
115	*TBX19*	0.000289	-1.171713	**147**	*NR2F2*	0.003781	-1.126786	**179**	*MDFI*	0.000211	-1.082027
116	*KIAA1772*	0.000644	-1.170781	**148**	*OR2B2*	0.001187	-1.123974	**180**	*APBB1IP*	0.000054	-1.079027
117	*SPRR2C*	0.000877	-1.169085	**149**	*HOXC4*	0.006499	-1.123726	**181**	*OR51S1*	0.005369	-1.070911
118	*MS4A7*	0.000484	-1.168639	**150**	*C20orf195*	0.001963	-1.12343	**182**	*SPANXN2*	0.004563	-1.070139
119	*SLC37A2*	0.000183	-1.167494	**151**	*RPS10P7*	0.001896	-1.123268	**183**	*ITGAM*	0.000097	-1.068902
120	*G6PC*	0.001687	-1.167205	**152**	*RBP7*	0.009865	-1.120622	**184**	*PROKR1*	0.000271	-1.067033
121	*DEFB123*	0.005833	-1.165392	**153**	*IGSF6*	0.00041	-1.119765	**185**	*ASPA*	0.037009	-1.065427
122	*LINC00602*	0.000498	-1.164531	**154**	*EME2*	0.019056	-1.117081	**186**	*FSTL3*	0.000155	-1.063874
123	*EBI3*	0.00006	-1.164307	**155**	*SUSD3*	0.000155	-1.114983	**187**	*FCER1G*	0.000026	-1.062954
124	*C20orf54*	0.000031	-1.164201	**156**	*OR10H2*	0.00048	-1.113771	**188**	*LOC643421*	0.0057	-1.062897
125	*HMGCS2*	0.000047	-1.162735	**157**	*APOD*	0.00086	-1.11244	**189**	*NR5A2*	0.002631	-1.059087
126	*C1orf226*	0.000111	-1.160511	**158**	*PATE3*	0.000078	-1.110198	**190**	*ACCN3*	0.002279	-1.059046
127	*AIF1*	0.000061	-1.160064	**159**	*TBC1D3*	0.000648	-1.108674	**191**	*AGXT2L1*	0.000443	-1.058594
128	*LYVE1*	0.000264	-1.158721	**160**	*CSNK1A1L*	0.029286	-1.108302	**192**	*DIRC1*	0.00052	-1.057317

Supplementary Table 3. Overview of GO terms for down-regulated genes that remained significant after BH correction

GO term	Description	P-value	FDR q-value	Enrichment (N, B, n, b)
GO:0098883	synapse pruning	2.73E-08	2.56E-04	18.00 (3402,6,189,6)
GO:0002478	antigen processing and presentation of exogenous peptide antigen	2.20E-07	1.03E-03	7.50 (3402,24,189,10)
GO:0019884	antigen processing and presentation of exogenous antigen	3.49E-07	1.09E-03	7.20 (3402,25,189,10)
GO:0042116	macrophage activation	3.61E-07	8.49E-04	9.60 (3402,15,189,8)
GO:0048002	antigen processing and presentation of peptide antigen	5.39E-07	1.01E-03	6.92 (3402,26,189,10)
GO:0019882	antigen processing and presentation	1.76E-06	2.75E-03	6.21 (3402,29,189,10)
GO:0002269	leukocyte activation involved in inflammatory response	1.99E-06	2.67E-03	12.00 (3402,9,189,6)
GO:0001774	microglial cell activation	1.99E-06	2.34E-03	12.00 (3402,9,189,6)
GO:0002504	antigen processing and presentation of peptide or polysaccharide antigen via MHC class II	3.60E-06	3.77E-03	9.00 (3402,14,189,7)
GO:0002495	antigen processing and presentation of peptide antigen via MHC class II	3.60E-06	3.39E-03	9.00 (3402,14,189,7)
GO:0002504	antigen processing and presentation of peptide or polysaccharide antigen via MHC class II	3.60E-06	3.77E-03	9.00 (3402,14,189,7)
GO:0002495	antigen processing and presentation of peptide antigen via MHC class II	3.60E-06	3.39E-03	9.00 (3402,14,189,7)
GO:0019886	antigen processing and presentation of exogenous peptide antigen via MHC class II	3.60E-06	3.08E-03	9.00 (3402,14,189,7)
GO:0061900	glial cell activation	4.74E-06	3.71E-03	10.80 (3402,10,189,6)
GO:0002376	immune system process	5.95E-06	4.30E-03	1.83 (3402,491,189,50)
GO:0002685	regulation of leukocyte migration	7.27E-06	4.89E-03	4.18 (3402,56,189,13)
GO:0150062	complement-mediated synapse pruning	9.24E-06	5.80E-03	18.00 (3402,4,189,4)
GO:0019221	cytokine-mediated signaling pathway	1.76E-05	1.03E-02	2.51 (3402,172,189,24)
GO:0006955	immune response	2.04E-05	1.13E-02	2.07 (3402,295,189,34)
GO:0002274	myeloid leukocyte activation	3.17E-05	1.66E-02	2.89 (3402,112,189,18)
GO:0002252	immune effector process	4.18E-05	2.07E-02	2.39 (3402,181,189,24)
GO:0002281	macrophage activation involved in immune response	4.42E-05	2.08E-02	14.40 (3402,5,189,4)
GO:0002281	macrophage activation involved in immune response	4.42E-05	2.08E-02	14.40 (3402,5,189,4)
GO:0006911	phagocytosis, engulfment	5.61E-05	2.51E-02	7.71 (3402,14,189,6)
GO:0002682	regulation of immune system process	5.73E-05	2.45E-02	1.88 (3402,363,189,38)
GO:0002275	myeloid cell activation involved in immune response	6.43E-05	2.63E-02	2.97 (3402,97,189,16)
GO:0002366	leukocyte activation involved in immune response	6.51E-05	2.55E-02	2.75 (3402,118,189,18)
GO:0002263	cell activation involved in immune response	6.51E-05	2.45E-02	2.75 (3402,118,189,18)
GO:0045321	leukocyte activation	6.58E-05	2.38E-02	2.32 (3402,186,189,24)
GO:0001775	cell activation	7.11E-05	2.48E-02	2.22 (3402,211,189,26)
GO:0099024	plasma membrane invagination	8.93E-05	3.00E-02	7.20 (3402,15,189,6)
GO:0010324	membrane invagination	8.93E-05	2.90E-02	7.20 (3402,15,189,6)
GO:0097242	amyloid-beta clearance	1.01E-04	3.16E-02	9.00 (3402,10,189,5)
GO:0071404	cellular response to low-density lipoprotein particle stimulus	1.27E-04	3.85E-02	12.00 (3402,6,189,4)
GO:1902563	regulation of neutrophil activation	1.27E-04	3.73E-02	12.00 (3402,6,189,4)
GO:0150064	vertebrate eye-specific patterning	1.69E-04	4.81E-02	18.00 (3402,3,189,3)
GO:2000416	regulation of eosinophil migration	1.69E-04	4.67E-02	18.00 (3402,3,189,3)

Supplementary Table 4. Overview of the cell-type enrichment analysissignificant after BH correction

Cell-type	Markers	P-value	Benjamini-Hochberg p-value	Odds Ratio
Deactivated microglia	95	3.630e-05	0.001	7.07
Oligodendrocyte	1	0.003	0.036	12.38
Microglia	30	0.06	0.53	2.87
Astrocyte	1	1	1	0.42
Basket	9	1	1	27.15
Bergmann	7	1	1	1.33
Brainstem Cholin	1	1	1	27.15
Cerebellar granule cells	42	1	1	4.28
Dentate Granule	5	1	1	5.43
Dopaminergic	3	1	1	27.15
Ependymal	6	1	1	0.96
Forebrain Cholinergic	1	1	1	7.40
GabaPV	4	1	1	11.63
GabaReln	5	1	1	6.26
GabaRelnCalb	1	1	1	27.15
GabaSSTReln	4	1	1	9.05
GabaVIPReln	10	1	1	7.40
Gluta	119	1	1	27.15
Gogli	85	1	1	9.05
Hypocretinergic	103	1	1	3.88
Activated microglia	8	0.27	1	1.97
Noradrenergic	23	1	1	4.79
Purkinje	27	0.28	1	3.15
Pyramidal	1	1	1	27.15
Serotonergic	6	1	1	6.26
Spinal Cord Cholinergic	6	1	1	6.26
Spiny	10	1	1	3.88
Thalamus Cholinergic	16	1	1	2.47

References

1. Alonso, G., 2000. Prolonged corticosterone treatment of adult rats inhibits the proliferation of oligodendrocyte progenitors present throughout white and gray matter regions of the brain. *Glia 31* (3), 219–231.
2. Amaya, J.M., Suidgeest, E., Sahut-Barnola, I., Dumontet, T., Montanier, N., Keller, C., Meijer, O.C., 2021. Effects of long-term endogenous corticosteroid exposure on brain volume and glial cells in the AdKO mouse. Front. *Neurosci. 15*, 604103.
3. Andela, C.D., van der Werff, S.J.A., Pannekoek, J.N., van den Berg, S.M., Meijer, O.C., van Buchem, M.A., Pereira, A.M., 2013. Smaller grey matter volumes in the anterior cingulate cortex and greater cerebellar volumes in patients with long-term remission of Cushing's disease: a case-control study. *Eur. J. Endocrinol. 169* (6), 811–819.
4. Bas-Hoogendam, J.M., Andela, C.D., van der Werff, S.J.A., Pannekoek, J.N., van Steenbergen, H., Meijer, O.C., Pereira, A.M., 2015. Altered neural processing of emotional faces in remitted Cushing's disease. *Psychoneuroendocrinology 59*, 134–146.
5. Beck, A.T., Epstein, N., Brown, G., Steer, R.A., 1988. An inventory for measuring clinical anxiety: psychometric properties. J. Consult. *Clin. Psychol. 56* (6), 893–897.
6. Benjamini, Y., Hochberg, Y., 1995. Controlling the false discovery rate: a practical and powerful approach to multiple testing. *J. R. Stat. Soc. Ser. B Methodol. 57* (1), 289–300.
7. Broadbent, D.E., Cooper, P.F., FitzGerald, P., Parkes, K.R., 1982. The cognitive failures questionnaire (CFQ) and its correlates. *Br. J. Clin. Psychol. 21* (1), 1–16.
8. Chapuis, J., Hot, D., Hansmannel, F., Kerdraon, O., Ferreira, S., Hubans, C., Ayral, A.M., 2009. Transcriptomic and genetic studies identify IL-33 as a candidate gene for Alzheimer's disease. Mol. *Psychiatry 14* (11), 1004–1016.
9. Chatterjee, A., Anderson, K.E., Moskowitz, C.B., Hauser, W.A., Marder, K.S., 2005. A comparison of Self-report and caregiver assessment of depression, apathy, and irritability in Huntington's disease. *J. Neuropsychiatry Clin*. *Neurosci. 17* (3), 378–383.
10. Chen, H., He, Y., Ji, J., Shi, Y., 2019. A machine learning method for identifying critical interactions between gene pairs in Alzheimer's disease prediction. F*ront. Neurol.* 10.
11. Chen, J., Bardes, E.E., Aronow, B.J., Jegga, A.G., 2009. ToppGene Suite for gene list enrichment analysis and candidate gene prioritization. *Nucleic Acids Res. 37* (Suppl_2), W305–W311.
12. Collins, D.L., Zijdenbos, A.P., Kollokian, V., Sled, J.G., Kabani, N.J., Holmes, C.J., Evans, A.C., 1998. Design and construction of a realistic digital brain phantom. IEEE Trans. *Med. Imaging 17* (3), 463–468.
13. De Kloet, E.R., Jo¨els, M., Holsboer, F., 2005. Stress and the brain: from adaptation to disease. Nat. Rev. *Neurosci. 6* (6), 463–475.
14. Dorn, L.D., Burgess, E.S., Dubbert, B., Simpson, S.E., Friedman, T., Kling, M., Chrousos, G.P., 1995. Psychopathology in patients with endogenous Cushings-syndrome - atypical or melancholic features. *Clin. Endocrinol. 43* (4), 433–442.
15. Drelon, C., Berthon, A., Sahut-Barnola, I., Mathieu, M., Dumontet, T., Rodriguez, S., Pointud, J.C., 2016. PKA inhibits WNT signalling in adrenal cortex zonation and prevents malignant tumour development. *Nat. Commun. 7* (1), 1–14.
16. Eden, E., Navon, R., Steinfeld, I., Lipson, D., Yakhini, Z., 2009. GOrilla: a tool for discovery and visualization of enriched GO terms in ranked gene lists. *BMC Bioinform. 10* (1), 1–7.
17. Forget, H., Lacroix, A., Somma, M., Cohen, H., 2019. Cognitive decline in patients with Cushing's syndrome (vol 6, pg 20, 2000). *J. Int. Neuropsychol. Soc. 6* (3), 375. https://doi.org/10.1017/S1355617700633155.
18. Fraile, J.M., Campos-Iglesias, D., Rodríguez, F., Espa˜nol, Y., Freije, J.M., 2016. The deubiquitinase USP54 is overexpressed in colorectal cancer stem cells and promotes intestinal tumorigenesis. *Oncotarget 7* (46), 74427–74434.

19. Franco, R., Fernandez-Suarez, D., 2015. Alternatively activated microglia and macrophages in the central nervous system. *Prog. Neurobiol. 131,* 65–86.
20. Guerreiro, R., Wojtas, A., Bras, J., Carrasquillo, M., Rogaeva, E., Majounie, E., Hazrati, L., 2013. TREM2 variants in Alzheimer's disease. *N. Engl. J. Med. 368* (2), 117–127.
21. Hawrylycz, M., Miller, J.A., Menon, V., Feng, D., Dolbeare, T., Guillozet-Bongaarts, A.L., Glasser, M.F., 2015. Canonical genetic signatures of the adult human brain. *Nat. Neurosci. 18* (12), 1832–1844.
22. Hawrylycz, M.J., Lein, E.S., Guillozet-Bongaarts, A.L., Shen, E.H., Ng, L., Miller, J.A., Abajian, C., 2012. An anatomically comprehensive atlas of the adult human brain transcriptome. *Nature 489* (7416), 391–399.
23. Heid, I.M., Jackson, A.U., Randall, J.C., Winkler, T.W., Qi, L., Steinthorsdottir, V., Workalemahu, T., 2010. Meta-analysis identifies 13 new loci associated with waist-hip ratio and reveals sexual dimorphism in the genetic basis of fat distribution. *Nat. Genet. 42* (11), 949–960.
24. Huntenburg, J.M., Bazin, P.L., Margulies, D.S., 2018. Large-scale gradients in human cortical organization. *Trends Cogn. Sci. 22* (1), 21–31.
25. Jin, H., Rugira, T., Ko, Y.S., Park, S.W., Yun, S.P., Kim, H.J., 2020. ESM-1 overexpression is involved in increased tumorigenesis of radiotherapy-resistant breast cancer cells. *Cancers 12* (6), 1363.
26. Jonsson, T., Stefansson, H., Steinberg, S., Jonsdottir, I., Jonsson, P.V., Snaedal, J., Rujescu, D., 2013. Variant of TREM2 associated with the risk of Alzheimer's disease. *N. Engl. J. Med. 368* (2), 107–116.
27. Juszczak, G.R., Stankiewicz, A.M., 2018. Glucocorticoids, genes and brain function. Prog. Neuropsychopharmacol. Biol. Psychiatry 82, 136–168. K´arad´ottir, R., Attwell, D., 2007. Neurotransmitter receptors in the life and death of oligodendrocytes. *Neuroscience 145* (4), 1426–1438.
28. Keo, A., Aziz, N.A., Dzyubachyk, O., van der Grond, J., van Roon-Mom, W., Lelieveldt, B. P., Mahfouz, A., 2017. Co-expression patterns between ATN1 and ATXN2 coincide with brain regions affected in Huntington's disease. *Front. Mol. Neurosci. 10*, 399.
29. Leccia, F., Batisse-Lignier, M., Sahut-Barnola, I., Val, P., Lefrançois-Martinez, A., Martinez, A., 2016. Mouse models recapitulating human adrenocortical tumors: what is lacking? *Front. Endocrinol. 7*, 93.
30. Lehmann, D.J., Wiebusch, H., Marshall, S.E., Johnston, C., Warden, D.R., Morgan, K., Welsh, K.I., 2001. HLA class I, II & III genes in confirmed late-onset Alzheimer's disease. *Neurobiol. Aging 22* (1), 71–77.
31. Leon-Carrion, J., Atutxa, A.M., Mangas, M.A., Soto-Moreno, A., Pumar, A., Leon-Justel, A., Leal-Cerro, A., 2009. A clinical profile of memory impairment in humans due to endogenous glucocorticoid excess. *Clin. Endocrinol. 70* (2), 192–200. https://doi.org/10.1111/j.1365-2265.2008.03355.x.
32. Li, C., Geng, H., Ji, L., Ma, X., Yin, Q., Xiong, H., 2019. ESM-1: a novel tumor biomarker and its research advances. *Anti-Cancer Agents Med. Chem. 19 (*14), 1687–1694.
33. Lin, Y.J., Liao, W.L., Wang, C.H., Tsai, L.P., Tang, C.H., Chen, C.H., Chen, J.H., 2017. Association of human height-related genetic variants with familial short stature in Han Chinese in Taiwan. *Sci. Rep. 7* (1), 1–7.
34. Mancarci, B.O., Toker, L., Tripathy, S.J., Li, B., Rocco, B., Sibille, E., Pavlidis, P., 2017. Cross-laboratory analysis of brain cell type transcriptomes with applications to interpretation of bulk tissue data. *eNeuro 4* (6).
35. Mantovani, A., Sica, A., Sozzani, S., Allavena, P., Vecchi, A., Locati, M., 2004. The chemokine system in diverse forms of macrophage activation and polarization. *Trends Immunol. 25* (12), 677–686.
36. Marks, I.M., Mathews, A.M., 1979. Brief standard self-rating for phobic patients. *Behav. Res. Ther. 17* (3), 263–267.

37. Martinez, F.O., Sica, A., Mantovani, A., Locati, M., 2008. Macrophage activation and polarization. *Front. Biosci. 13*, 453–461.
38. McQuade, A., Kang, Y.J., Hasselmann, J., Jairaman, A., Sotelo, A., Coburn, M., Danhash, E., 2020. Gene expression and functional deficits underlie TREM2-knockout microglia responses in human models of Alzheimer's disease. *Nat. Commun. 11* (1), 1–17.
39. Michaud, K., Forget, H., Cohen, H., 2009. Chronic glucocorticoid hypersecretion in Cushing's syndrome exacerbates cognitive aging. *Brain Cogn. 71* (1), 1–8. https:// doi.org/10.1016/j.bandc.2009.02.013.
40. Miyata, S., Koyama, Y., Takemoto, K., Yoshikawa, K., Ishikawa, T., Taniguchi, M., Tohyama, M., 2011. Plasma corticosterone activates SGK1 and induces morphological changes in oligodendrocytes in corpus callosum. *PLoS One 6* (5), e19859.
41. Montgomery, S.A., Åsberg, M.A.R.I.E., 1979. A new depression scale designed to be sensitive to change. B*r. J. Psychiatry 134* (4), 382–389.
42. Newell-Price, J., Bertagna, X., Grossman, A.B., Nieman, L.K., 2006. Cushing's syndrome. Lancet 367 (9522), 1605–1617. https://doi.org/10.1016/S0140-6736(06)68699-6.
43. Nieman, L.K., Ilias, I., 2005. Evaluation and treatment of Cushing's syndrome. *Am. J. Med. 118* (12), 1340–1346. https://doi.org/10.1016/j.amjmed.2005.01.059.
44. Nimmerjahn, A., Kirchhoff, F., Helmchen, F., 2005. Resting microglial cells are highly dynamic surveillants of brain parenchyma in vivo. *Science 308* (5726), 1314–1318.
45. Parkhurst, C.N., Yang, G., Ninan, I., Savas, J.N., Yates III, J.R., Lafaille, J.J., Gan, W.B., 2013. Microglia promote learning-dependent synapse formation through brain-derived neurotrophic factor. *Cell 155* (7), 1596–1609.
46. Pereira, A.M., Tiemensma, J., Romijn, J.A., 2010. Neuropsychiatric disorders in Cushing's syndrome. *Neuroendocrinology 92*, 65–70.
47. Pĩnero, J., Bravo, `A., Queralt-Rosinach, N., Gutĩerrez-Sacrisťan, A., Deu-Pons, J., Centeno, E., Furlong, L.I., 2016. DisGeNET: a comprehensive platform integrating information on human disease-associated genes and variants. *Nucleic Acids Res. 45*, gkw943.
48. Pivonello, R., De Leo, M., Cozzolino, A., Colao, A., 2015. The treatment of Cushing's disease. *Endocr. Rev. 36* (4), 385–486.
49. Ragnarsson, O., Berglund, P., Eder, D.N., Johannsson, G., 2012. Long-term cognitive impairments and attentional deficits in patients with Cushing's disease and cortisol-producing adrenal adenoma in remission. *J. Clin. Endocrinol. Metab. 97* (9), E1640–E1648.
50. Rush, A.J., Giles, D.E., Schlesser, M.A., Fulton, C.L., Weissenburger, J., Burns, C., 1986. The inventory for depressive symptomatology (IDS): preliminary findings. *Psychiatry Res. 18* (1), 65–87.
51. Saijo, K., Glass, C.K., 2011. Microglial cell origin and phenotypes in health and disease. *Nat. Rev. Immunol. 11* (11), 775–787.
52. Salter, M.W., Beggs, S., 2014. Sublime microglia: expanding roles for the guardians of the CNS. *Cell 158* (1), 15–24.
53. Seo, E.H., Kim, H.J., Kim, J.H., Lim, B., Park, J.L., Kim, S.Y., Kim, Y.S., 2020. ONECUT2 upregulation is associated with CpG hypomethylation at promoter-proximal DNA in gastric cancer and triggers ACSL5. *Int. J. Cancer 146* (12), 3354–3368.
54. Šerý, O., Goswami, N., Balcar, V.J., 2020. CD36 gene polymorphisms and Alzheimer's disease. Genetics, Neurology, Behavior, and Diet in Dementia. *Academic Press*, pp. 57–70.
55. Šerý, O., Janoutov´a, J., Ewerlingov´a, L., H´alov´a, A., Lochman, J., Janout, V., Balcar, V.J., 2017. CD36 gene polymorphism is associated with Alzheimer's disease. *Biochimi 135*, 46–53.
56. Smith, S.M., Jenkinson, M., Woolrich, M.W., Beckmann, C.F., Behrens, T.E.J., Johansen-Berg, H., Matthews, P.M., 2004. Advances in functional and structural MR image analysis and implementation as FSL. *NeuroImage 23*, S208–S219.
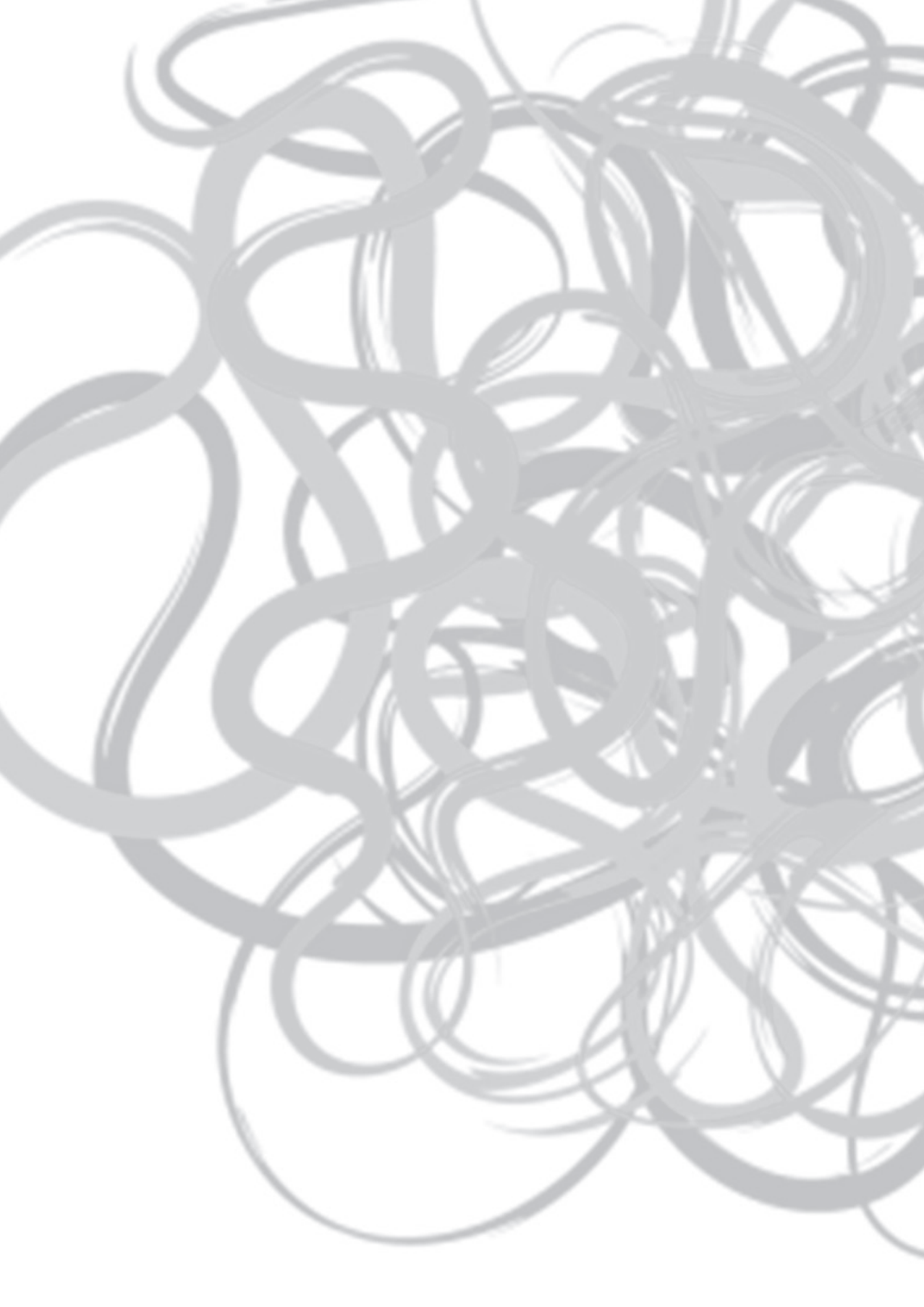
57. Sonino, N., Boscaro, M., Fallo, F., Fava, G.A., 2000. A clinical index for rating severity in Cushing's syndrome. Psychother. *Psychosom. 69* (4), 216–220.
58. Sonino, N., Fava, G.A., 2001. Psychiatric disorders associated with Cushing's syndrome – epidemiology, pathophysiology and treatment. *CNS Drugs 15* (5), 361–373. https://doi.org/10.2165/00023210-200115050-00003.
59. Starkman, M.N., Schteingart, D.E., Schork, M.A., 1986. Cushing's syndrome after treatment: changes in cortisol and ACTH levels, and amelioration of the depressive syndrome. *Psychiatry Res. 19* (3), 177–188.
60. Starkstein, S.E., Petracca, G., Chemerinski, E., Kremer, J., 2001. Syndromic validity of apathy in Alzheimer's disease. *Am. J. Psychiatry 158* (6), 872–877.
61. Shen, M., Dong, C., Ruan, X., Yan, W., Cao, M., Pizzo, D., Wang, S.E., 2019. Chemotherapy induced extracellular vesicle miRNAs promote breast cancer stemness by targeting ONECUT2. *Cancer Res. 79* (14), 3608–3621.
62. Shulman, J.M., Imboywa, S., Giagtzoglou, N., Powers, M.P., Hu, Y., Devenport, D., Brown, N.H., 2014. Functional screening in Drosophila identifies Alzheimer's disease susceptibility genes and implicates Tau-mediated mechanisms. *Hum. Mol. Genet. 23* (4), 870–877.
63. Starossom, S.C., Mascanfroni, I.D., Imitola, J., Cao, L., Raddassi, K., Hernandez, S.F., Wang, Y., 2012. Galectin-1 deactivates classically activated microglia and protects from inflammation-induced neurodegeneration. *Immunity 37* (2), 249–263.
64. Tiemensma, J., Kokshoorn, N.E., Biermasz, N.R., Keijser, B.J.S.A., Wassenaar, M.J.E. Middelkoop, H.A.M., Romijn, J.A., 2010. Subtle cognitive impairments in patientwith long-term cure of Cushing's disease. J. Clin. Endocrinol. *Metab. 95* (6), 2699–2714.
65. van der Werff, S.J.A., Andela, C.D., Pannekoek, J.N., Meijer, O.C., van Buchem, M.A., Rombouts, S.A.R.B., van der Wee, N.J.A., 2014. Widespread reductions of white matter integrity in patients with long-term remission of Cushing's disease. *NeuroImage Clin. 4*, 659–667.
66. van Weert, L.T., Buurstede, J.C., Mahfouz, A., Braakhuis, P.S., Polman, J.A.E., Sips, H.C., Roozendaal, B., Balog, J., de Kloet, E.R., Datson, N.A., Meijer, O.C., 2017. NeuroD factors discriminate mineralocorticoid from glucocorticoid receptor DNA binding in the male rat brain. *Endocrinology 158* (5), 1511–1522.
67. Wang, Z.X., Wan, Y., Tan, L., Liu, J., Wang, H.F., Sun, F.R., Yu, J.T., 2017. Genetic association of HLA Gene variants with MRI brain structure in Alzheimer's disease. *Mol. Neurobiol. 54* (5), 3195–3204.
68. Willette, A.A., Coe, C.L., Colman, R.J., Bendlin, B.B., Kastman, E.K., Field, A.S., Johnson, S.C., 2012. Calorie restriction reduces psychological stress reactivity and its association with brain volume and microstructure in aged rhesus monkeys. *Psychoneuroendocrinology 37* (7), 903–916.
69. Xu, H., Chen, X., Huang, Z., 2019. Identification of ESM1 overexpressed in head and neck squamous cell carcinoma. *Cancer Cell Int. 19* (1), 118.
70. Yao, Y., Huang, W., Li, X., Li, X., Qian, J., Han, H., Zhao, H., 2018. Tespa1 deficiency dampens thymus-dependent B-cell activation and attenuates collagen-induced arthritis in Mice. *Front. Immunol. 9*, 965.
71. Yao, Y., Zhang, H., Shao, S., Cui, G., Zhang, T., Sun, H., 2015. Tespa1 is associated with susceptibility but not severity of rheumatoid arthritis in the Zhejiang Han population in China. *Clin. Rheumatol. 34* (4), 665–671.
72. Zhang, L., Zhang, J., You, Z., 2018. Switching of the microglial activation phenotype is a possible treatment for depression disorder. *Front. Cell. Neurosci. 12*, 306.
73. Zheng, Z.V., Wong, K.C.G., 2019. Microglial activation and polarization after subarachnoid hemorrhage. Neuroimmunol. *Neuroinflamm. 6,* 1–10.